THE ASTROPHYSICAL JOURNAL, 459:L1–L4, 1996 March 1

CONFIRMATION OF HIGH DEUTERIUM ABUNDANCE IN QUASAR ABSORBERS

M. RUGERS AND C. J. HOGAN
University of Washington, Department of Astronomy, Box 351580, Seattle, WA 98195-1580
Received 1995 September 29; accepted 1995 December 22

ABSTRACT

We present a new analysis of a Keck spectrum of Q0014+813, with a new model of the $z = 3.32$ absorbing cloud. We fit Lyman series absorption of the dominant H I components, including components identified with hydrogen and associated deuterium at two discrete velocities, with thermal line broadening of each species. The deuterium features are too narrow to be interlopers, and the good agreement in temperature and redshift with their hydrogen counterparts confirms the identification as deuterium. The abundance is measured to be $D/H = (1.9 \pm 0.5) \times 10^{-4}$ and $(1.9 \pm 0.4) \times 10^{-4}$ in the two components, with an independent lower limit of $D/H > 1.3 \times 10^{-4}$ for the sum, derived from the Lyman limit opacity. The impact on cosmological theory is briefly discussed.

Subject headings: cosmology: observations — quasars: individual (0014+813)

1. CONFIRMING DEUTERIUM

The hydrogen cloud at redshift $z = 3.32$ along the line of sight to the quasar Q0014+813, shown by Chaffee et al. (1985, 86) to be uniquely well suited for measuring primordial abundances, was found recently to show an absorption feature at the precise wavelength predicted for cosmic deuterium (Songaila et al. 1994, hereafter SCHR; Carswell et al. 1994). The implied D/H abundance ratio from this feature, although it fits very well into the big bang predictions for primordial abundances (Copi, Schramm, & Turner 1995a; Dar 1995; Fields & Olive 1996; Olive et al. 1996), is much higher than that usually derived from models of Galactic chemical evolution normalized by solar system ^{3}He abundances (Galli et al. 1995; Wilson & Rood 1994; Hata et al. 1995; Copi et al. 1995b), and also much higher than the best estimate of D/H in another QSO absorber, on the line of sight to Q1937−1009 (Tytler & Fan 1994). The simplest explanation of this discrepancy is that the feature in Q0014+0813 is not caused by deuterium at all, but is simply a low-column density hydrogen cloud that happens to lie at a somewhat different velocity from the bulk of the local hydrogen, at the redshift expected for deuterium (SCHR; Steigman 1994). Although the redshift coincidence is quite precise (± 5 km s^{-1}), the chance of such a coincidence is still not negligible, and was estimated to be at least a few percent, ignoring possible correlations.

We can eliminate the possibility of interlopers even in a single system if the candidate D lines are very narrow. The line width, characterized by the Doppler parameter in a thermal profile fit, $b \equiv (2kT/m)^{1/2}$, is $13T_4^{1/2}$ km s^{-1} for hydrogen and $9T_4^{1/2}$ km s^{-1} for deuterium. The potential interloper population is observed to have lines below $b = 20$ km s^{-1} only very rarely (Hu et al. 1995), so a narrower line is much more naturally identified with deuterium than with a chance interloper. Also, in very narrow lines, thermal broadening is likely to dominate the line width, so the ratio of the fitted Doppler parameter for D candidates to their H counterparts is an important clue. Here we use evidence from line shapes to confirm the identification of the deuterium features and sharpen the estimate of the primordial deuterium abundance.

2. OBSERVATIONS AND REDUCTION

We use the same data described in SCHR: six exposures of 40 minutes each were obtained of Q0014+813, at the Keck telescope on 1993 November 11 using the HiRes echelle spectrograph with a $1\farcs2 \times 3\farcs8$ slit. A resolution $R = 36{,}000$ was obtained over the covered wavelength range of 3500 to 6080 Å. Unlike SCHR, the raw data were reduced using IRAF. The CCD frames were overscan corrected, bias subtracted, and flat fielded using CCDPROC. After verifying the registration of the frames, the frames were then stacked using IMSUM, with rejection of the highest pixel value among the frames, in order to reject cosmic rays. Fewer cosmic rays were left using this method than by creating a median with IMCOM. The stacked images were then used for extraction of the individual orders of the spectrum using DOECSLIT, where the standard star frame was used to trace the orders on the CCD and ThAr calibration lamp data were used to obtain the wavelength calibration. No attempts were made to flux calibrate the spectrum. The resulting extracted, dispersion-corrected echelle spectrum was then run through RVCORRECT to obtain the correction for radial velocity of the observer with respect to the QSO, so redshifts quoted here are in vacuo, relative to the local standard of rest. The data were not smoothed, as they were in SCHR; the new results presented here are due primarily to using the full instrumental resolution of the raw data.

3. MODEL FITS FOR H I AND D I

After examining the Lyman series of this absorber complex, we decided to use Lyα, Lyβ, Lyγ, Lyδ, Lyζ, and Lyκ through 17 for establishing fits. Lyε was thrown out due to the presence of significant absorption from Lyα-forest interlopers. A value for $\log N_{\rm H\,I}$ of 17.3 (estimated from the Lyman limit optical depth) was used as an initial guideline for the column density of the bluest part of the complex, where most of the H I is located, as is shown by the higher order lines. The code used to perform the model fits to the spectrum is VPFIT, which models the formation of an absorption spectrum as a series of thermally broadened components at discrete velocities (Carswell et al. 1987; Webb 1987). For each component, VPFIT determines

TABLE 1

VPFIT RESULTS FOR THE ABSORBERS IN FIGURE 1

Component	Ion	log N	±	z	±	b (km s^{-1})	±
1	H I	15.45	0.68	2.310923	0.000015	22.1	4.3
2	H I	13.18	0.09	2.644001	0.000052	25.0	6.5
3	H I	13.22	0.11	2.648422	0.000038	16.8	5.7
4	H I	13.71	0.04	2.649057	0.000025	24.7	3.0
5	H I	12.78	0.34	3.315725	0.000309	34.3	12.4
6	H I	13.24	0.12	3.316360	0.000029	17.6	3.5
7	H I	14.01	0.07	3.317390	0.000050	25.3	2.9
8	H I	14.28	0.05	3.318026	0.000028	19.6	2.2
9	H I	12.99	0.42	3.318726	0.000388	38.0	12.9
10	H I	13.74	0.34	3.320050	0.000064	10.4	5.0
11	D I	13.03	0.10	3.320483	0.000010	7.5	1.2
12	H I	16.76	0.07	3.320482	0.000044	10.1	2.0
13	D I	13.18	0.07	3.320789	0.000012	8.8	1.1
14	H I	16.90	0.06	3.320790	0.000037	12.7	0.8
15	H I	15.22	0.38	3.321300	0.000131	13.1	4.3
16	H I	16.36	0.16	3.322225	0.000041	22.8	2.1
17	H I	15.36	0.19	3.322955	0.000088	17.8	6.0
18	H I	14.44	0.32	3.323513	0.000089	12.0	5.1
19	H I	13.06	0.13	3.324024	0.000078	24.0	6.4

the redshift (z), Doppler parameter (b), and column density (N) by fitting the data with Voigt profiles convolved with a Gaussian instrument profile, and makes formal error estimates from the covariance matrix parameters, for each of the calculated z, b, and N, based on the reduced χ^2. (Note that although these are "true" 1 σ errors, including the total fitting uncertainty in each parameter, the probability distribution is highly non-Gaussian, so they do not translate directly into "confidence intervals." The results quoted in SCHR were used as a starting point for the fits performed by VPFIT.

The Doppler parameter for the D component fitted to the smoothed data by SCHR, 14 km s^{-1} (assuming thermal broadening only), is too large for a good fit to the unsmoothed data. A narrower fit is required both by the steep profile edge of the D feature at the blue side of this absorber complex, and by a sharp spike in the center, which may at first sight appear to be noise. However, since in the top part of this spike there are three channels, each of which has between 6 and 7 σ counts above the bottom of the absorption dip, this is statistically very unlikely to be a noise feature. The feature also appears if the same data are reduced using the independent software used by SCHR, indicating it is not due to the different procedure performed here (A. Songaila 1995, private communication). A much better fit was obtained using two H I absorbers instead of one, each of which has a log $N_{\rm H\,I}$ of around 16.8, both with corresponding D I absorption lines. This two-component fit is also preferred by the H I lines on their own, without the split D Lyα feature; by adding the three new parameters corresponding to the one new H I component, the reduced χ^2 per degree of freedom for the best fit is equal to 0.98, instead of the 6.1 obtained for the best fit with only one main H I hydrogen absorber. This is mainly due to the improved fit in the higher Lyman series lines.

The best overall fit was obtained by the components as presented in Table 1, where the components of interest for the deuterium abundance are numbers 11 to 14. Figure 1 shows plots of the data and the fit to Lyα through Lyδ, plus Lyζ, all plotted on the same velocity scale. Most interloper features in the higher orders were omitted from the fit. Some areas of poorly fitted excess flux in Lyδ and Lyζ must be due to artifacts or noise, as corresponding flux does not appear in higher orders. The highest order line fits are shown in Figure 2. Although many parameters of the minor components are not well determined by the fit, as they are convolved with higher column density lines in the regions where they are optically thin, the H I columns of the dominant components (12 and 14) are well constrained by the line fits in the unsaturated high Lyman series, and the D I columns are well determined by the unsaturated Lyα lines, so the absolute deuterium abundances can be estimated fairly accurately.

The D/H ratios for both of the main absorbers are in good agreement with each other, as well as with the value obtained by SCHR. For the $z = 3.320482$ absorber, we find D/H = $10^{-3.73\pm0.12}$, and for the $z = 3.320790$ absorber, we find D/H = $10^{-3.72\pm0.09}$, where we have added the errors in log $N_{\rm H\,I}$ and log $N_{\rm D\,I}$ in quadrature. We therefore expect the D/H ratio for these absorbers to lie within the ranges of $1.9^{+0.6}_{-0.5} \times 10^{-4}$ and $1.9^{+0.5}_{-0.4} \times 10^{-4}$, respectively. The total D column is $(2.6 \pm 0.4) \times 10^{13}$, which also gives D/H = $(1.9 \pm 0.4) \times 10^{-4}$ when compared to total hydrogen column in the two main absorbers. These are consistent with the estimates made by SCHR and Carswell et al. (1994), using lower resolution.

The total $N_{\rm H\,I}$ in the two main absorbers from this fit is $(1.37 \pm 0.16) \times 10^{17}$ (the errors here obtained by adding in quadrature the errors for each), which agrees with the total $N_{\rm H\,I}$ of the whole absorber complex estimated from the Lyman break. This can be seen qualitatively in Figure 2, from the good match of the fitted absorber model at the Lyman limit to the regions of highest flux shortward of the limit. The flux beyond the Lyman limit can be used to derive an upper limit for the total hydrogen column in the absorber complex, which yields a fairly stringent lower limit on the D/H ratio independent of H I line fits. In order to try and circumvent any leftover instrument effects in this part of the spectrum, the continuum of the QSO and the standard star were assumed to have the same shape over this narrow range (50 Å), and the shape of the standard star continuum was fitted to match the parts of the QSO spectrum at the red end of the order, in regions without conspicuous absorption. This gave an estimate for the continuum level, which was used both for the high-order line fit and the continuum level beyond the Lyman limit, and appears at the blue end of the fit in Figure 2. The level of the signal beyond the Lyman limit was estimated in two ways. The simplest of these used the mean of the counts per channel, blueward of the Lyman limit in this order. This gives an upper limit to the opacity of the cloud complex, and hence an upper limit to the total hydrogen column of the cloud, which can be used to find a very conservative lower limit to the D/H ratio of the two absorbers. The second uses the mean of only those regions blueward of the Lyman limit where the counts per channel are at least 1 σ above the zero level, over a range of at least 1 Å. Two examples are the regions around 3932 and 3941 Å, each of which is a few angstroms wide. Since additional Lyα and Lyman limit absorption must still occur in these areas, the value for the opacity determined from this estimate of the Lyman limit signal is also an upper limit. The two methods yield upper limits to the total H I column density of 2.4×10^{17} and 1.7×10^{17} cm^{-2}, respectively.

This limit almost exactly matches the sum of all the fitted components (including in particular number 16 in Table 1 in addition to the two main components), so there is almost no room to hide more than a small fraction of additional H I anywhere in this complex beyond that already accounted for in the fits. Taking the lower limit on D to be 2.2×10^{13} cm^{-2},

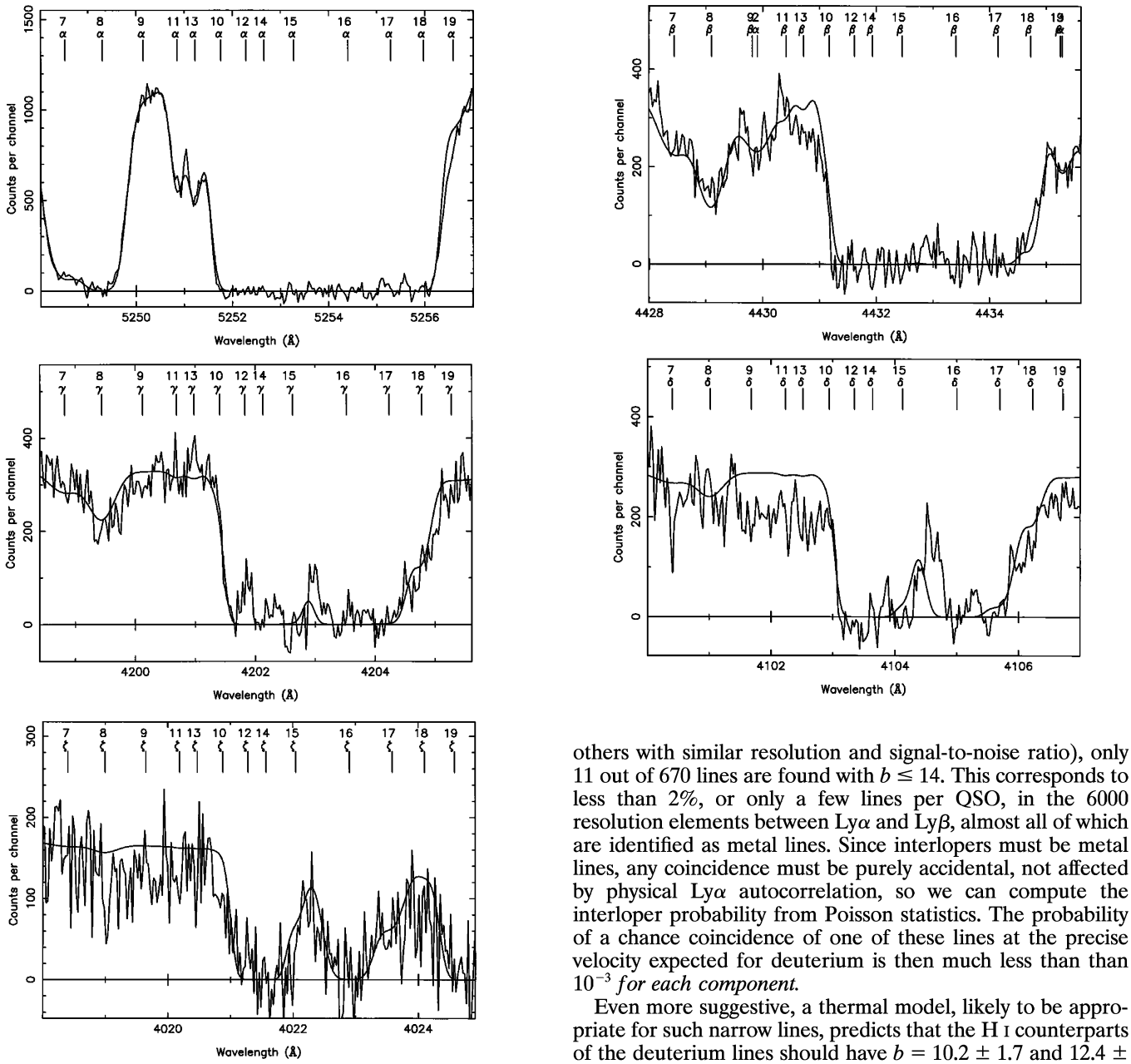

FIG. 1.—Spectral fits to Lyα, Lyβ, Lyγ, Lyδ, and Lyζ, plotted on the same velocity scale. Ticks mark the centroids of individual components, with parameters tabulated in Table 1; the overall model fit comprising the sum of this absorption is the solid line. The ticks corresponding to the bulk of the hydrogen column, and their deuterium counterparts, are systems numbered 12/14 and 11/13, respectively.

which is well constrained by the unsaturated D Lyα, therefore yields a firm lower limit D/H $\geq 1.3 \times 10^{-4}$, in good accordance with the lower limits determined from the hydrogen line fits. Therefore, if the D candidate lines are indeed caused by deuterium, D/H must be high.

Most significantly for confirmation of deuterium, the D I lines are narrow, making the interloper possibility very unlikely. The fits for the two components are 7.5 ± 1.2 and 8.8 ± 1.1 km s^{-1}. Hu et al. (1995) find that in three QSOs (including this one, using the same data we are using, and others with similar resolution and signal-to-noise ratio), only 11 out of 670 lines are found with $b \leq 14$. This corresponds to less than 2%, or only a few lines per QSO, in the 6000 resolution elements between Lyα and Lyβ, almost all of which are identified as metal lines. Since interlopers must be metal lines, any coincidence must be purely accidental, not affected by physical Lyα autocorrelation, so we can compute the interloper probability from Poisson statistics. The probability of a chance coincidence of one of these lines at the precise velocity expected for deuterium is then much less than than 10^{-3} *for each component.*

Even more suggestive, a thermal model, likely to be appropriate for such narrow lines, predicts that the H I counterparts of the deuterium lines should have $b = 10.2 \pm 1.7$ and 12.4 ± 1.6 km s^{-1}, in agreement with the observed values of $b = 10.1 \pm 2.0$ and 12.7 ± 0.8 km s^{-1}. This coincidence also argues against random interlopers.

In fact, the H I lines are unusually narrow for forest lines, but this is not surprising since this system was selected for high column density, which often goes with low ionization parameter and temperature. We also examined the data to look for metal absorption lines, but found only upper limits for C II, C III, Si II, and Si III, all species with several lines in regions of the spectrum that are unobstructed by interlopers, and that have reasonable S/N. These results are nevertheless consistent with a sensible physical model of the main absorbing clouds. Using the models of Donahue & Shull (1991), we adopt a conservative limit on the ionization parameter for the gas log $U \lesssim -4$ (where $U = n_\gamma/n_{\rm H}$), which gives an equilibrium temperature limit $T_4 \leq 1.2$ consistent with the narrow width of the H and D features. This gives a neutral fraction of the hydrogen

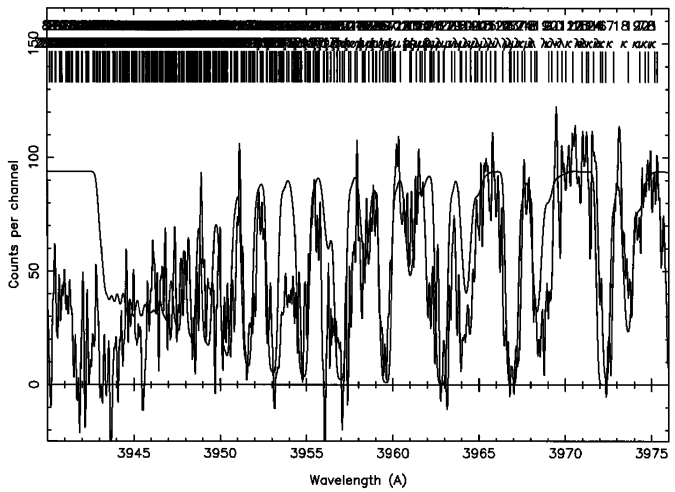

FIG. 2.—Spectral fit of the same absorption model to Lyman 10 through 17. The data in the plot (but not the fit) has been boxcar averaged at 7 km s^{-1} to reduce noise. The plotted model does not include photoelectric continuum absorption and recovers beyond the limit to the QSO continuum; the predicted continuum from the line absorption model is the asymptotic value of the line fit curve longward of the break, which agrees with the observed flux beyond the limit.

of $\gtrsim 3 \times 10^{-2}$, and estimated C and Si abundances $\lesssim 10^{-3}$ solar. With such a small ionization parameter ($U \ll 10^{-2}$), charge-exchange reactions $D^+ + H \rightleftharpoons D + H^+$ guarantee that H and D are locked to the same fractional ionization (J. Black 1995, private communication), so $N_{D\,I}/N_{H\,I}$ indeed gives the true deuterium abundance of the gas.

4. DISCUSSION

These results reinforce the interpretation of the candidate deuterium features in Q0014+813 as deuterium associated with the hydrogen. First, instead of one component, we now have two cases where the H and D velocities agree. A second coincidence is that both components give the same abundance—that is, the estimated D I columns of the individual components are in the same ratio as the columns of H I. The third coincidence is that the width of both D I features agrees with that predicted for D I at the same temperature as the hydrogen. Finally and most significantly, if the features are interlopers, they are too narrow to be part of the numerous Lyα forest and therefore need to be two of the much rarer narrow and uncorrelated metal line population, making the probability of two chance interlopers at the precise required velocities vanishingly small. By contrast, the deuterium interpretation makes good physical sense, and provides a natural explanation of all of these coincidences.

The low metal abundance makes it seem unlikely that more than a small fraction of the gas has been processed through stars, so that a negligible fraction of the initial deuterium has been destroyed. Since the big bang is the only known source of deuterium (Reeves et al. 1973), we may take the absorber abundance as our best estimate of the primordial abundance, $(D/H)_p = (1.9 \pm 0.4) \times 10^{-4}$. Standard big bang nucleosynthesis (SBBN) then gives a baryon-to-photon ratio $\eta = (1.7 \pm 0.2) \times 10^{-10}$, corresponding to $\Omega_b h^2 = (6.2 \pm 0.8) \times 10^{-3}$. For this value of η, SBBN predictions are consistent with estimates of cosmic ^{4}He and ^{7}Li abundances (Copi et al. 1995a, b; Hata et al. 1995; Dar 1995; Fields & Olive 1996). The total baryon density is then only about 3 times larger than the cosmic density of known baryons in gas and stellar populations (Persic & Salucci 1992), allowing a tidy picture where most cosmic baryons reside in or near galaxies and clusters of galaxies rather than in a dominant, diffuse intergalactic medium (Fukugita, Hogan, & Peebles 1996). There are not enough extra baryons to make most of the dark matter in galaxy halos, consistent with the constraints from MACHO observations (Alcock et al. 1995), and implying that the bulk of galactic dark matter is nonbaryonic.

Our estimated primordial deuterium abundance is much larger than that of the Milky Way (Linsky et al. 1995), probably due to burning in stars, which converts it to ^{3}He. The low value of ^{3}He inferred in the presolar nebula and found in parts of the interstellar medium (Wilson & Rood 1994) can be explained as further conversion of the ^{3}He to heavier elements in stars (Hogan 1995; Wasserburg, Boothroyd, & Sackmann 1995; Charbonnel 1995; Weiss, Wagenhuber, & Denissenkov 1996; Olive et al. 1996), rather than as a low primordial value of deuterium.

We are particularly grateful to A. Songaila and L. L. Cowie for performing the observations and sharing the data, R. Carswell for use of his VPFIT software and for help in using it, to the staff at NOAO, in particular, F. Valdez, for help with IRAF, and to J. Black, S. Burles, C. Foltz, G. Wallerstein, A. Wolfe, and the referee for helpful suggestions. This work was supported at the University of Washington by NSF grant AST 932 0045.

REFERENCES

Alcock, C., et al. 1995, Phys. Rev. Lett., 74, 2867
Carswell, R. F., Webb, J. K., Baldwin, J. A., & Atwood, B. 1987, ApJ, 319, 709
Carswell, R. F., Rauch, M., Weymann, R. J., Cooke, A. J., & Webb, J. K. 1994, MNRAS, 268, L1
Chaffee, F. H., Foltz, C. B., Röser, H.-J., Weymann, R. J., & Latham, D. W. 1985, ApJ, 292, 362
Chaffee, F. H., Foltz, C. B., Bechtold, J., & Weymann, R. J. 1986, ApJ, 301, 116
Charbonnel, C. 1995, ApJ, 453, L41
Copi, C. J., Schramm, D. N., & Turner, M. S. 1995a, Science, 267, 192
———. 1995b, Phys. Rev. Lett., 75, 3981
Dar, A. 1995, ApJ, 449, 550
Donahue, M., & Shull, J. M. 1991, ApJ, 383, 511
Fields, B. D., & Olive, K. A. 1996, Phys. Lett. B., in press
Fukugita, M., Hogan, C. J., & Peebles, P. J. E. 1996, Nature, in press
Galli, D., Palla, F., Ferrini, F., & Penco, U. 1995, ApJ, 443, 536
Hata, N., Scherrer, R. J., Steigman, G., Thomas, D., Walker, T. P., Bludman, S., & Langacker, P. 1995, Phys. Rev. Lett., 75, 3977
Hogan, C. J. 1995, ApJ, 441, L17
Hu, E. M., Kim, T.-S., Cowie, L. L., & Songaila, A. 1995, AJ, 110, 1526
Linsky, J. L., Diplas, A., Wood, B. E., Brown, A., Ayres, T. R., & Savage, B. D. 1995, ApJ, 451, 335
Olive, K. A., Rood, R. T., Schramm, D. N., Truran, J. W., & Vangioni-Flam, E. 1995, ApJ, 444, 680
Persic, M., & Salucci, P. 1992, MNRAS, 258, 148
Reeves, H., Audouze, J., Fowler, W. A., & Schramm, D. N. 1973, ApJ, 179, 909
Songaila, A., Cowie, L. L., Hogan, C. J., & Rugers, M. 1994, Nature, 368, 599 (SCHR)
Steigman, G. 1994, MNRAS, 269, L53
Tytler, D., & Fan, X. M. 1994, BAAS, 26, 4, 1424
Wasserburg, G. J., Boothroyd, A. I., & Sackmann, I.-J. 1995, ApJ, 447, L37
Webb, J. K. 1987, Ph.D. thesis, Cambridge Univ.
Weiss, A., Wagenhuber, J., & Denissenkov, P. A. 1996, A&A, in press
Wilson, T. R., & Rood, R. T. 1994, ARA&A, 32, 191